Data analysis challenges in gravitational-wave astronomy

Éric Chassande-Mottin for the LIGO Scientific Collaboration and the Virgo Collaboration

APC, Univ Paris Diderot, CNRS/IN2P3, CEA/Irfu, Obs de Paris, Sorbonne Paris Cité, France

Abstract. Gravitational waves are radiative solutions of space-time dynamics predicted by Einstein's theory of General Relativity. A world-wide array of large-scale and highly-sensitive interferometric detectors constantly scrutinizes the geometry of the local space-time with the hope to detect deviations that would sign an impinging gravitational wave from a remote astrophysical source. Finding the rare and weak signature of gravitational waves buried in non-stationary and non-Gaussian instrument noise is a particularly challenging problem. We will give an overview of the data-analysis techniques and associated observational results obtained so far by Virgo (in Europe) and LIGO (in the US), along with the prospects offered by the upcoming advanced versions of those detectors.

Einstein's theory of General Relativity introduces the concept of a deformable and evolving space-time. The dynamics of space-time is prescribed by the Einstein equation. In the linearized gravity which assumes small deformations in a nearly flat space-time, this equation reduces to the wave equation which therefore evidences the existence of radiative solutions. The latter are referred to as *gravitational waves* (GW) and can phenomenologically seen as propagating disturbances of space-time itself. The theory also predicts that GW are transverse waves, that they nominally propagate at the speed of light and possess two independent polarizations [1, 2].

GW have never been directly detected i.e., through the measurement of their effect on a man-made instrument. Strong evidence of their existence has been provided by the observation of the famous Hulse-Taylor pulsar binary (PSR B1913+16) [3]. The decay rate of the binary orbital period is in remarkable agreement with the predicted evolution obtained under the assumption that this system radiates energy away in the form of GW.

The direct search for GW made notable progresses with the advent of dedicated instruments based on high-precision laser interferometry such as LIGO and Virgo (see [4, 5] for a detailed review). With the ongoing installation of new and improved generation of those instruments, the first discovery seem to be only a few years away.

While electromagnetic waves are produced by accelerated charges, GW are produced by accelerated masses. Very large masses and relativistic velocities are necessary to generate GW at a detectable level. For this reason, the current projects aiming at detecting GW target potential astrophysical sources involving very dense and compact objects such as neutron stars or black holes. Very

energetic astrophysical events such as the coalescence of neutron star and/or black holes binaries, or stellar core collapses are expected to be the source of intense and short-duration bursts of GW [4].

Because of the limited rate of occurrence for such events, searching for such transient GW in the LIGO and Virgo data essentially consists in searching for rare and weak signals at the detectability limit. This article gives the state-of-the-art of the search for GW transient signals with a focus on the related data analysis challenges. We first give some introductory material with a general presentation of the detectors in Sec. 1 and an review of the relevant astrophysical sources in Sec. 2. Sec. 3 gives an overview the major problems faced when searching for transient GW along with the data analysis methods deployed to address them.

1. INTERFEROMETRIC GW DETECTORS

The first generation of interferometric GW detectors comprises six large-scale instruments in total (see Fig. 1). The US-based Laser Interferometer Gravitational-Wave Observatory (LIGO) [6] includes three kilometric-scale instruments located in Livingston, Louisiana (labelled L1) and Hanford, Washington (the latter hosting two interferometers in the same vacuum enclosure with labels H1 and H2). The French-Italian project Virgo [7] has one instrument of the same class located in Cascina near Pisa, Italy (labelled V1). This set of kilometer-scale instruments is complemented by a detector with more modest dimensions (several hundreds of meters): GEO [8], a German-British detector in operation near Hanover, Ger-

FIGURE 1. Geographic location of the current and future GW interferometric detectors. The future detector LIGO-India is still pending approval and its exact location is yet to be determined. Credits: [9]

FIGURE 2. (top) Time line of the data takings completed so far. Credits: [10] **(bottom) Sensitivity achieved by LIGO and Virgo during their last science data taking S6/VSR2**.

many.

Despite major differences in the technologies in use, all those instruments measure gravitational waves through the same principle. They all sense the strain that a passing GW exerts on space-time by monitoring the differential length $\delta \ell$ of the optical path followed by two laser beams propagating along orthogonal directions over a distance L. This is performed by letting the two beams used for the measurement interfere similarly to the Michelson-Morley experiment. The interference is closely related to the difference in the phase accumulated by the two beams before they combine and hence to the difference in their optical paths. The measurement of the interference light power allows that of $\delta \ell$ with high accuracy. Measurement noises (mainly the thermal noise due to the Brownian agitation of the atoms constitutive of the optics and the shot noise due to the quantum nature of light) can be reduced to reach the level of $h \equiv \delta \ell / L \sim 10^{-21}$, where h is detector response, homogeneous to the a-dimensional GW amplitude. The best sensitivity is achieved in a frequency band ranging from ~ 100 Hz to 1 kHz approximately (see Fig. 2 – bottom).

The detector response is a linear mixture $h = F_+ h_+ + F_\times h_\times$ of the two GW polarizations h_+ and $h_\times$. The antenna pattern factors F_+ and $F_\times$ characterize the way the wave polarizations couple to the detector. The coupling $\mathscr{F} = (F_+^2 + F_\times^2)^{1/2} \leq 1$ is maximum for waves coming from the normal to the detector plane and is minimum (and exactly zero) for waves from the four "blind" directions associated to the two bisectors of the detector arms. GW detectors are non-directional instruments as $\mathscr{F} \gtrsim 1/2$ for more than half of the sky.

The first generation detectors have conducted a series of science data takings reaching an integrated volume of about 2 years (see Fig. 2 – top). The data takings are coordinated in order to maximize the observation time with the three most sensitive detectors operating while always maintaining at least one detector in "astro-watch"
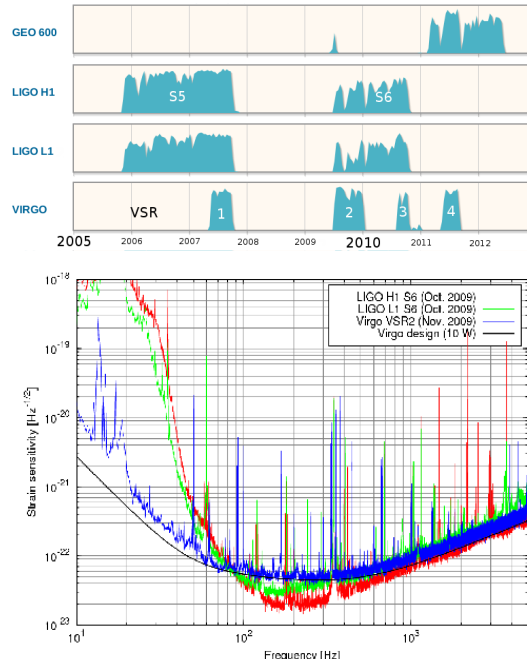
mode in case of an outstanding galactic event.

The first generation of detectors have now been decommissioned and it is currently being replaced by a second generation of "advanced" detectors. Thanks to major upgrades in their infrastructure and instrumentation, a ten-fold increase in sensitivity is expected with the advanced detectors as indicated in Fig. 3. The GW amplitude decaying inversely with the distance, this corresponds to a factor of thousand in the observable volume of Universe and hence in the number of detectable sources. Advanced detectors are likely to detect several and possibly several tenths of sources as we will see in the next Section.

The installation of the advanced LIGO detectors [11] should be completed by the end of 2013 and a first science run is expected to take place in 2015. The original plan was to install two four-kilometer detectors at Hanford site, but there is now a proposal (still to be approved by U.S. and Indian institutions) to move one of those detectors at a new observatory in India. It this plan materializes, the third detector at the Indian site would start operation around 2020. Advanced Virgo plans to have a robustly operating detector in 2015 and to begin collecting science data as soon as possible after that [12]. GEO foresees a program of upgrades "GEO-HF" [13] which focuses on improving the detector sensitivity at high-frequencies thanks to a larger laser power and the
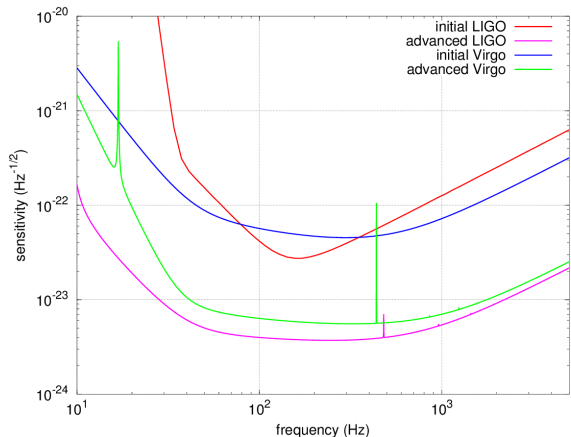
FIGURE 3. Projected sensitivities for the advanced LIGO and advanced Virgo detectors compared with the design sensitivity of their initial version.

FIGURE 4. Example of the expected GW waveform from the coalescence of a black-hole binary as predicted by the post-Newtonian theory. Credits: [18]

used of "squeezed light". The network of advanced detectors will be completed by the Japanese KAGRA detector [14] which has the specificity of being installed underground in the Kamioka mine (where the seismic motion is much lower than at the surface) and to operate at cryogenic temperature to reduce thermal noise. An initial three-kilometer room-temperature interferometer is expected to be operational by 2015, with the full cryogenic interferometer ready to start taking data by 2018.

2. ASTROPHYSICAL SOURCES OF GW TRANSIENTS

Phenomenologically, GW emission arises from relativistic bulk motion. At lowest order, GW can be related to variations in the quadrupolar moment of the mass distribution [1]. Therefore, GW sources have to present some degree of non-axisymmetry. In this section, we review the astrophysical scenarios giving rise to GW emission. The coalescence of neutron-star and/or black-hole binaries similar to the Hulse-Taylor binary mentioned previously is often considered the most promising one.

The last minutes before the system merges give rise to the emission of an intense burst of GW. Post-Newtonian expansions of the binary dynamics [15, 16] are used to predict the gravitational waveforms radiated during the inspiral phase which precedes the merger. The GW signature consists in a *chirp* signal whose frequency sweeps toward high values according to a power law at first order (see Fig. 4 for an example). A substantial amount of energy is radiated in the following phase when the two bodies merges into a black-hole. In this highly relativistic phase, the perturbative treatment of binary dynamics is not valid anymore and one has to resort to numeri-
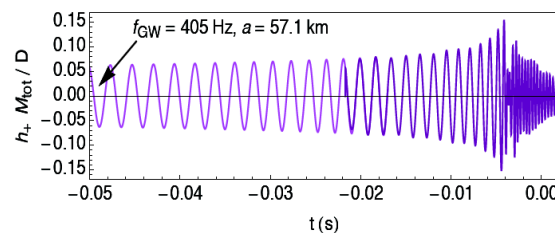
cal simulations. The process is concluded by the ringdown phase during which the resulting distorted blackhole radiates away its asymmetry down to equilibrium. It is estimated that during the whole coalescence process, a stellar-mass binary radiates away about a percent of its rest mass. The fraction of mass loss grows to $\gtrsim 10\%$ for more massive binary black-hole systems.

Although binary systems are fairly common, only a small fraction eventually forms a compact binary that is sufficiently tight to coalesce in less than Hubble time. A survey of population estimates [17] gives a "realistic" rate of one neutron-star–neutron-star coalescence[1] per 10,000 year per galaxy equivalent in size to the Milky Way. Converted into a rate of *detectable* coalescences, this leads to ~ 0.02 events per year with the first generation of (initial) detectors and to ~ 40 events for the second generation (advanced). Large error bars are attached to those estimates reflecting the weakness of the observation constraints we have about those systems. The above stated rates can then be 10 times smaller or larger in the "pessimistic" or "optimistic" respectively. The "realistic" rates presented above are corroborated by the ones derived assuming that compact binary mergers are the progenitors of short-hard gamma-ray bursts (GRB).

Gravitational stellar-core collapse is another potential source of GW if some degree non-axisymmetry is exhibited during this process. The simulations required to make reliable predictions of the emission levels are very challenging as they have to incorporate many physical ingredients including relativistic magneto-hydrodynamics and a detailed treatment of neutrino transport and nuclear iterations [19]. The current realistic estimate of the amount of radiated GW energy is of order $10^{-7} M_\odot$ and corresponds approximately [20] to a distance reach of order ~ 10 kpc with the initial detectors, ~ 100 kpc with the advanced detectors. The detectable sources are therefore located in the Galaxy.

---

[1] Similar rates are obtained for the other types of systems mixing neutron-stars and/or black-holes.

Another potential source of GW bursts are "neutron-star quakes" [21] during which the vibrational normal modes of a neutron-star are excited and damped by GW emission. Star quakes may origin from the disruption of the star crust due to the sudden rearrangement of the magnetic field of a highly-magnetized neutron-star (magnetar). Cosmic string cusps may be also listed among the potential GW burst sources [22].

3. SEARCHES FOR GW TRANSIENT SIGNALS

3.1. Time-series analysis

In detection problems, the availability of *a priori* information plays a major rôle. We have seen in Sec. 2 that the GW signature from coalescing binaries of neutron stars and/or black holes have a specific time evolution which can be predicted with good accuracy. This morphological information helps to distinguish a real GW signal from the instrumental or environmental noise. The search for known signals is efficiently performed by *matched filtering techniques* [23] which cross-correlates the data with the expected "template" waveforms obtained from the source model.

Because of the highly-relativistic dynamics associated with the production of GW, some of the expected GW waveforms are difficult to predict with accuracy. This calls for detection methods that are robust to the model uncertainties. *Excess power methods* essentially consists in searching for a broad family of GW waveforms by scanning a time-frequency map for transient excursions. The time-frequency map is obtained by projecting the data onto a dictionary of elementary waveforms that tiles the time-frequency plane. Several types of dictionary have been tested including local cosines [24], sine-Gaussian wavelets [25], orthogonal wavelet packet bases [26] or chirplets [27]. Real GW signals are unlikely to correlate exactly with one element in the dictionary, but with several of them. Clustering algorithms are generally applied to harvest the signal energy scattered over several elements [28, 29, 30].

The time-frequency dictionaries mentioned above are composed of "generic" elementary waveforms mainly motivated by mathematical or algorithmic arguments. Astrophysically motivated dictionaries can be obtained by extracting the relevant information from catalogs of GW signals developed through numerical simulations [31, 32, 33, 34].

3.2. Multi-detector analysis

We described the basic ideas employed to analyze the data stream from individual detector. A gain in sensitivity is expected from the availability of joint observation by multiple detectors. This section discusses several aspects related to the combined analysis of multiple detector data.

3.2.1. Coherent analysis of multiple data stream

We already mentioned that the detector receives a mixture of both GW polarizations which depends on the relative orientation and alignment of the detector and wave. Since the detectors are not co-planar and co-aligned, they couple differently to the incoming wave resulting in observed responses with different initial phases and amplitudes. Because of its finite speed, GW reaches the detectors at different times. All those differences can be exploited using *coherent analysis techniques* to improve the overall sensitivity. Those techniques consists in compensating the phase shift and delay of the various responses to align them in time and phase assuming a given direction-of-arrival. The resulting data stream are combined so that the sum operates constructively for GW signals from the selected direction. The data stream which results from the coherent combining maximizes the signal-to-noise ratio (SNR). The combined stream can be then analyzed using methods inspired from the single detector case, i.e., excess power methods for the unmodelled GW bursts [35, 36] and matched filtering techniques [37, 38] for inspiralling binaries. The coherent analysis being directional (each coherently combined stream is associated to a given direction), the outcome is a probability (pseudo-)distribution over the sky usually referred to *sky map* from which the most likely location of the source can be extracted.

3.2.2. Mitigation of non-Gaussian/non-stationary noise

The noise of the real instruments is far from the ideal properties of stationarity and Gaussianity we expect from the main fundamental (thermal and quantum) noises. It is dominated by an overwhelming component of non-Gaussian non-stationary noises consisting in a large number of transient noise excursions commonly called *glitches*. Glitches are produced by a variety of environmental and instrumental processes, such local seismic noise or saturations in feedback control systems. Since glitches occasionally occur nearly simultaneously in separate detectors by chance, they can mimic a gravitational-wave signal.

The population of glitches are difficult to model. The size and the large complexity of GW detectors makes this modelling even more difficult. GW detectors being extended instruments over kilometers, it is hard to completely isolate them from the outside world and the surrounding anthropic activity. Therefore, the accurate modelling of the non-Gaussian/non-stationary noise background is for now out-of-reach. It has to be mitigated and this can be done at least partially by using multiple data.

It is possible to calculate combinings of the data from multiple detectors where the GW signals from all detectors interfere destructively in the sum. The GW signal thus cancels, but not background glitches. The energy in these "null" stream(s) may be used to reject or downweight events not consistent with a gravitational wave [39, 36]. The success of such tests depend critically on having several independent detectors of comparable sensitivity.

3.2.3. Use of multiple data for background estimation

We explained earlier that the accurate modelling of non-Gaussian non-stationary noise is out-of-reach. The remaining part of the glitches that cannot be identified by the coherent techniques described in the previous section constitutes the dominating background noise in burst searches. This background has to be estimated. However, GW signals cannot be turned off: the detectors cannot be shielded from them. Therefore, we don't have "noise-only" data at disposal for background estimation.

Nevertheless, the background can be estimated thanks to the availability of multiple data streams by time shifting one detector's data. The time-shift is chosen to be much longer than the time-of-flight between detectors ($\sim$ 30 ms) and coherence time scale of the detector noise ($\sim$ seconds). Time-shifted (or "time slide") analysis only leave triggers due to accidental coincidences of instrumental glitches. The contribution from real GW signals is erased. By repeating the analysis many times with different time-shifts, we get an accurate estimate of the rate of background events. For sufficiently large time shifts, each trials can be considered independent to the other. However, the number of time-slides cannot be increased indefinitely as a significant correlation between time-slides will occur above a certain level [40].

The p-value measuring the significance of a GW event can be computed by computing the fraction of louder background events from the time-slide analysis.
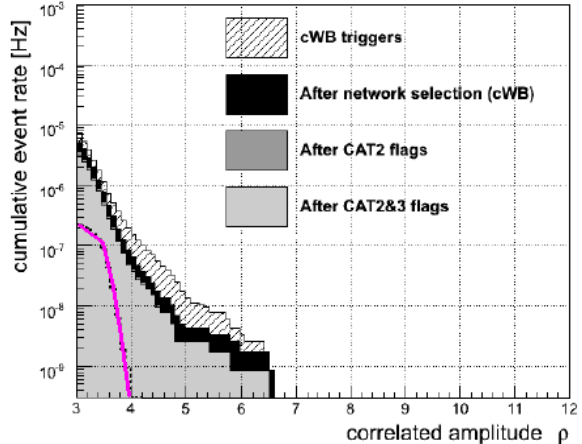

FIGURE 5. **Examples of background distributions for the coherent Wave-Burst algorithm [36] for a three-detector network (LIGO-H and L and Virgo) during S6-VSR2/3 data taking.** This distribution is given as a function of the correlated amplitude ρ homogeneous to the signal-to-noise ratio. **Hatch area**: background *before* any glitch rejection scheme is applied. **Black area**: *after* the "null-stream" glitch rejection (see Sec. 3.2.2). **Gray area**: *after* data-quality flags (see Sec. 3.3). CAT2 and 3 refers to the different categories of the data-quality flags whose description goes beyond the scope of this article. **Bold curve**: expectation if noise is stationary and Gaussian. Credits: [41].

3.3. Data quality

Besides the gravitational-wave channel $h(t)$, hundreds of auxiliary channels including microphones, seismometers, magnetometers, etc. are recorded at any given time during science data takings. Those channels can be used to get an image of the operational and environmental status of the detector. The observed correlation between the GW channel with the auxiliary channels can help determine the origin of noise artifacts and how the original disturbance couples into the detector [41]. A significant number of noise sources are identified *a posteriori* after the science data taking is done. Those noise sources cannot be mitigating by fixing the instrument. Instead, this leads to the development of a data-quality flag which when "raised" indicates that the data are improper, and any event occurring at that time should be *vetoed*. This provides also an important resource for background glitch rejection. Data-quality flags with a large ($\gg 1$) efficiency (percentage of glitches vetoed by the flag) over dead-time (fraction of science time rejected by the flag) ratio are particular interest [41]. About 200 data-quality flags are used in GW burst searches. Figure 5 shows the background improvement after vetoing.
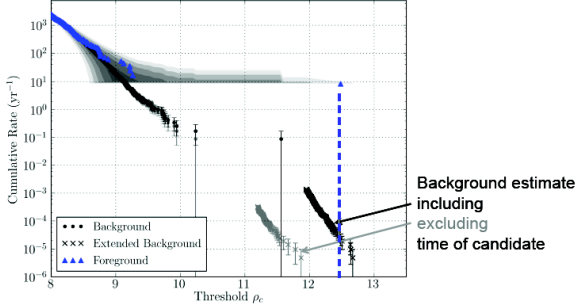
FIGURE 6. Cumulative event rate associated to the search for compact binary coalescences. Credits: [42]

3.4. Results

LIGO and Virgo conducted two joint science runs, labelled S5 for LIGO and VSR1 for Virgo for the first run, S6 and VSR2/3 for the second. A total of $T = 635$ days of observing time have been analyzed [43, 44]. No GW have been detected. Upper limit (at 50% confidence level) on the GW strain obtained from an all-sky all-time GW burst search have been set and it is slightly below $h_{rss} < 5 \times 10^{-22}$ $\text{Hz}^{-1/2}$ for waveform frequency at about 200 Hz, where the bound is on the root-square-sum amplitude $h_{rss}^2 \equiv \int dt\, h_+^2(t) + h_\times^2(t)$ of the two GW polarizations at Earth. Note that the exact result depends on the assumed GW model. The generic model of a sine Gaussian waveform characterized by its central frequency is assumed here.

This upper limit placed on a local quantity (h_{rss} at Earth) can be translated into astrophysical constraints. For instance, lower limits on the radiated energy E_{GW} by generic sources of linearly polarized GW located at distance d. Averaging over the source inclination, the above strain limit corresponds to $E_{GW} = 2 \times 10^{-8} M_\odot c^2$ for galactic sources at distance $d = 10$ kpc, and $E_{GW} = 5 \times 10^{-2} M_\odot c^2$ for source in the Virgo cluster with $d = 15$ Mpc. Those estimates are comparable to the expected GW-radiated energy from core collapses and mergers of stellar-mass compact objects respectively.

The same data, when searched specifically for inspiralling binaries of neutron stars, leads to an upper limit on the rate of such astrophysical events of $\mathscr{R}_{90\%} = 1.3 \times 10^{-4} \text{yr}^{-1} L_{10}^{-1}$ [45, 42] which is still two orders of magnitude larger than the rate estimate obtained from population models [17]. Fig. 6 shows the cumulative rate of events detected by the matched-filtering procedure outlined in Sec. 3.1 in coincidence in the H1 and L1 detectors during four months of S6/VSR2-3 data taking. This distribution is displayed as a function of the ranking statistic ρ_c which combines the signal-to-noise ratios measured at both detectors. The distribution of true events (triangle) is superimposed to a background esti-

mate (black dots) with error bars (in gray). The last triangle on the right-hand side of the plot at $\rho_c \approx 12.5$ is an event detected with false-alarm rate of 1 in 7,000 years [42]. It was known in advanced that a small number of fake GW signals might be added "blindly" to the data. The exact time and characteristics of these signals were only known by a small group of people sworn to silence until the eventual "opening of the envelop". The envelop was *not* empty and contained the detected event code-named GW100916 [18]. Thanks to this exercise, it was possible to test the entire decision-making chain leading to the publication of the detection.

4. ONLINE ANALYSIS AND RAPID ELECTROMAGNETIC FOLLOW-UP

Sources of GW are likely sources of other kinds of emissions, such as electromagnetic waves or jets of high-energy particles. The possible connection between compact binary coalescences and GRB is an example [46]. This motivates cross-correlating GW with other types of observations in the electromagnetic or neutrino spectra see e.g., [47, 48] for recent results. We will briefly report here on rapid follow-up observations seeking electromagnetic counterparts to GW candidate events. A low-latency analysis pipeline was operated for the first time during the last data taking [49]. It allows to generate alerts "on the fly" within 20 minutes of the associated GW candidate event. Major changes were required with respect to the original off-line pipelines. The most probable direction of the source along with an error box were communicated to a dozen of partner observatories [49] including radiotelescopes, wide-field optical telescopes and the X/gamma-rays satellite Swift. This has led to follow-up observations which have been scanned for transient excursions. This exercice has been extremely useful and will help to prepare the exciting future of multimessenger astronomy with the advanced detectors [50, 9].

ACKNOWLEDGMENTS

REFERENCES

1. K. Thorne, "Gravitational Radiation," in *300 Years of Gravitation*, edited by S. W. Hawking, and W. Israel, Cambridge University Press, 1987.

2. M. Maggiore, *Gravitational Waves – Volume 1: Theory and Experiments*, Oxford University Press, 2008.

3. J. M. Weisberg, D. J. Nice, and J. H. Taylor, *ApJ* **722**, 1030–1034 (2010), `arXiv:1011.0718`.

4. B. S. Sathyaprakash, and B. F. Schutz, *Living Rev. Rel.* **12** (2009).

5. K. Riles, Gravitational waves: Sources, detectors and searches (2012), to appear in Progress in Particle and Nuclear Physics, `arXiv:1209.0667`.

6. B. P. Abbott, et al., *Rept. Prog. Phys.* **72**, 076901 (2009), `arXiv:0711.3041`.

7. T. Accadia, et al., *Class. Quantum Grav.* **28**, 114002 (2011).

8. H. Grote for the LIGO Scientific Collaboration, *Class. Quantum Grav.* **27**, 084003 (2010).

9. P. S. Shawhan for the LIGO Scientific Collaboration and Virgo Collaboration, Rapid alerts for following up gravitational wave event candidates (2012), `arXiv:1206.6163`.

10. LIGO open science center (2012), `https://losc.ligo.org/timeline`.

11. G. M. Harry for the LIGO Scientific Collaboration, *Class. Quantum Grav.* **27** (2010).

12. F. Acernese, et al., Advanced Virgo baseline design, Tech. Rep. VIR-0027A-09, Virgo Collaboration (2010).

13. H. Lück, et al., *J. Phys. Conf. Ser.* **228** (2010).

14. K. Somiya for the KAGRA Collaboration, *Class. Quantum Grav.* **29** (2012).

15. L. Blanchet, *Living Rev. Rel.* **5**, 3 (2002), `gr-qc/0202016`.

16. A. Buonanno, G. B. Cook, and F. Pretorius, *Phys. Rev. D* **D75**, 124018 (2007), `gr-qc/0610122`.

17. J. Abadie, et al., *Class. Quantum Grav.* **27**, 173001–+ (2010).

18. GW100916 blind injection data release (2011), `http://www.ligo.org/science/GW100916`.

19. C. D. Ott, *Class. Quantum Grav.* **26**, 063001 (2009).

20. P. Sutton, A rule of thumb for the detectability of gravitational-wave bursts (2010), `https://dcc.ligo.org/cgi-bin/private/DocDB/ShowDocument?docid=10614`.

21. N. Chamel, and P. Haensel, *Living Reviews in Relativity* **11** (2008), `http://www.livingreviews.org/lrr-2008-10`.

22. X. Siemens, et al., *Phys. Rev. D* **D73**, 105001 (2006), `gr-qc/0603115`.

23. B. F. Schutz, *The detection of Gravitational Waves*, Cambridge University Press, Cambridge, England, 1991, chap. Data processing, analysis and storage for interferometric antennas, pp. 406–452, D. Blair, ed.

24. W. G. Anderson, et al., *Phys. Rev. D* **63**, 042003 (2001).

25. S. Chatterji, et al., *Class. Quantum Grav.* **21**, S1809–S1818 (2004), `gr-qc/0412119`.

26. S. Klimenko, et al., *Class. Quantum Grav.* **21**, S1685–S1694 (2004), `gr-qc/0407025`.

27. E. Chassande-Mottin, et al., *Class. Quantum Grav.* **27**, 194017 (2010), `arXiv:1005.2876`.

28. J. Sylvestre, *Phys. Rev. D* **66**, 102004 (2002).

29. R. Khan, and S. Chatterji, *Class. Quantum Grav.* **26**, 155009 (2009), `arXiv:0901.3762`.

30. E. Chassande-Mottin, and A. Pai, *Phys. Rev. D* **D73**, 042003 (2006), `gr-qc/0512137`.

31. I. S. Heng, *Class. Quantum Grav.* **26**, 105005 (2009), `arXiv:0810.5707`.

32. C. Rover, et al., *Phys. Rev. D* **D80**, 102004 (2009), `arXiv:0909.1093`.

33. P. R. Brady, and S. Ray-Majumder, *Class. Quantum Grav.* **21**, S1839–S1848 (2004), `gr-qc/0405036`.

34. E. Chassande-Mottin, *Phys. Rev. D* **D67**, 102001 (2003), `gr-qc/0210008`.

35. Y. Guersel, and M. Tinto, *Phys. Rev. D* **40**, 3884–3938 (1989).

36. S. Klimenko, et al., *Class. Quantum Grav.* **25**, 114029 (2008), `arXiv:0802.3232`.

37. I. Harry, and S. Fairhurst, *Class. Quantum Grav.* **28**, 134008 (2011), `1101.1459`.

38. A. Pai, S. Dhurandhar, and S. Bose, *Phys. Rev. D* **D64**, 042004 (2001), `gr-qc/0009078`.

39. S. Chatterji, et al., *Phys. Rev. D* **74**, 082005 (2006).

40. M. Was, et al., *Class. Quantum Grav.* **27**, 015005 (2010), `arXiv:0906.2120`.

41. J. Aasi, et al., *Class. Quantum Grav.* **29**, 155002 (2012), `arXiv:1203.5613`.

42. J. Abadie, et al., *Phys. Rev. D* **85**, 082002 (2012).

43. J. Abadie, et al., *Phys. Rev. D* **81**, 102001 (2010).

44. J. Abadie, et al., *Phys. Rev. D* **85**, 122007 (2012).

45. J. Abadie, et al., *Phys. Rev. D* **82**, 102001 (2010).

46. A. Corsi, "Gravitational waves and gamma-ray bursts," in *Proceedings of the International Astronomical Union*, Cambridge University Press, 2011, vol. 7, pp. 142–149.

47. J. Abadie, et al., Search for gravitational waves associated with gamma-ray bursts during LIGO science run 6 and Virgo science runs 2 and 3 (2012), to appear in ApJ, `arXiv:1205.2216`.

48. S. Adrian-Martinez, et al., A First Search for coincident Gravitational Waves and High Energy Neutrinos using LIGO, Virgo and ANTARES data from 2007 (2012), `arXiv:1205.3018`.

49. J. Abadie, et al., *A&A* **539** (2012).

50. LSC and Virgo policy on releasing gravitational wave triggers to the public in the advanced detectors era (2012), `https://dcc.ligo.org/cgi-bin/DocDB/ShowDocument?docid=89391`.